International Journal of Computer Information Systems and Industrial Management Applications
ISSN 2150-7988 Volume 18(13s) 2026 pp. 1085-1101
https://doi.org/10.70917/ijcisim-2026-4149
Article

An Optimization of Multiple Route Selection in Flying Ad Hoc Network

Shaleena H[1], Sumangala K[2]

[1]Department of Computer Science, Kongunadu Arts and Science College, Coimbatore, Tamil Nadu
[2]Department of Computer Applications, Kongunadu Arts and Science College, Coimbatore, Tamil Nadu
Corresponding Author: Shaleena H

Abstract: Routing in Flying Ad Hoc Networks (FANETs) poses challenges because of their dynamic topology and limited resources. Developing effective routing protocols (RPs) is essential to enhancing the network's Quality of Service (QoS). An example of such a protocol is the Multipath Energy-efficient and Predictive Fuzzy Logic with Consistent Link-based Copy Adaptive Transmit-based Routing Protocol (MEPFL-CLCT-RP), which utilizes backup paths based on link survival probabilities to improve the data communication and network performance. However, the protocol faces issues such as high complexity and routing overhead, particularly in environments with high mobility, which can affect scalability. This paper proposes a novel approach by incorporating the Hippopotamus Optimization Algorithm (HOA) with MEPFL-CLCT-RP for FANETs. The proposed HOA-MEPFL-CLCT-RP uses a Fuzzy Logic (FL) system to identify several suboptimal routes connecting the origin and target nodes. The HOA then ranks and selects the most reliable backup path by evaluating potential routes based on their link survival probability. This technique minimizes routing overhead and delays, ensuring smooth transitions to backup paths during link failures. Simulation results indicate that HOA-MEPFL-CLCT-RP outperforms existing models in terms of Packet Delivery Ratio (PDR), energy efficiency, End-to-End Delay (E2D), and routing overhead.
Keywords: FANET,Routing overhead,Multipath routing, HOA, Backup path

1. INTRODUCTION

The rapid advancement of Internet of Things (IoT) technologies has driven the widespread adoption of Unmanned Aerial Vehicles (UAVs). These UAVs have found applications across various domains, including logistics, aerial surveillance, disaster management, precision agriculture, public safety, and cybersecurity [1], [2]. UAVs can function either under remote control or autonomously, navigating predefined flight paths to perform specific tasks efficiently. FANETs represent the type of multi-hop wireless network that facilitates the seamless communication among UAVs [3]. They are designed to enhance network coverage, improve communication capacity, and enable flexible configurations without centralized infrastructure [4], [5]. FANETs support both single-UAV and multi-UAV systems. Single-UAV setups rely on Base Stations (BS) and satellites for communication, requiring intricate hardware integration [6]. In contrast, multi-UAV systems enhance reliability, resilience, and workload distribution by utilizing collaborative operations among multiple UAVs and satellites [7], [8].

FANETs utilize five primary communication methods, such as UAV-to-BS, BS-to-BS, UAV-to-UAV, UAV-to-Satellite, and UAV-to-Sensor. These methods support the exchange of data such as video feeds and sensor readings, enabling efficient communication between UAVs and other network entities [9]. Ad hoc interactions between UAVs enable localized data dissemination, while satellite links ensure long-range connectivity [10]. Because of their high mobility and changeable topology, FANETs have particular difficulties, including frequent connection failures, erratic communication paths, resource constraints, and vulnerability to network splitting [11]. To address these challenges, specialized RPs have been developed to meet the specific requirements of FANETs. Traditional ad hoc network protocols are often ineffective for UAV networks due to their rapid movement, three-dimensional mobility, and constrained resources [12]. Moreover, FANET applications exhibit varying QoS requirements, ranging from latency-tolerant tasks to real-time data transfer for mission-critical applications, such as security and emergency response [13].

Recent advancements in FANET RPs have aimed to reduce latency, minimize overhead, and improve stability [14]. For instance, the EPFL-based RP introduces mechanisms for path discovery and maintenance, leveraging FL to assess UAV stability, mobility, and energy efficiency [15]. Despite these innovations, traditional protocols often encounter challenges, such as increased routing overhead, delays, and inefficiencies in large-scale scenarios. To address these limitations, the MEPFL-CLCT-RP was introduced. This protocol employs link survival probabilities to select backup paths, enhancing reliability during link failures. However, MEPFL-CLCT-RP is constrained by its complexity and frequent monitoring requirements, which can strain resources in highly dynamic FANET environments [16].

1.1 Problem Definition

In FANETs, selecting backup paths for multi-path routing is crucial for network reliability. However, the MEPFL-CLCT-RP algorithm becomes more complex as it calculates the survival probability for each link and chooses the best backup path. The frequent monitoring and updating of these backup routes can lead to significant routing overhead, affecting network performance. This issue is especially challenging in dynamic FANET environments where UAVs frequently move, requiring more recalculations and updates. To address this issue, an optimization technique can be a more efficient alternative for choosing optimal backup paths and improving network performance.

1.2 Major Contributions

This study proposes the HOA-MEPFL-CLCT-RP, a novel approach for identifying the optimal backup path in multipath routing within FANETs. The primary objective of this protocol is to reduce routing overhead and transmission delays by selecting efficient paths based on factors such as link stability, energy consumption, and overall network performance. The main aspects of this framework are given below.

- Utilizing an FL system approach to identify several possible pathways between the origin and target points, ensuring optimal route choice.
- Employing a multicast strategy for Route Request (RREQ) and Route Reply (RREP) messages. The HOA evaluates each candidate backup path’s fitness based on its link survival probability and identifies the most reliable path.
- Providing a seamless mechanism for handling link failures. When a link breaks, the source node leverages the backup path selected by HOA for data transfer. Alternatively, if another valid route exists, the CLCT method ensures data transmission by duplicating packets across available paths.
- Streamlining the process of establishing new routes in dynamic FANET environments, thereby minimizing routing overhead and delays. HOA ensures that the selected backup path consistently delivers optimal performance under changing network conditions.

1.3 Paper Outline

The paper is organized as follows: Section 2 discusses previous research and recent developments in FANET routing protocols. The complete illustration of the proposed work is explained in Section 3. Section 4 presents the experimental outcomes and assesses the protocol's performance. Section 5 wraps up the study and suggests potential avenues for future work.

2. LITERATURE SURVEY

In this paper, recent studies related to the RPs in FANETs are discussed. Arafat and Moh [17] introduced QTAR, a Q-learning-based RP for FANETs. 2-hop data from UAV nodes was used to manage network topology and select optimal routes based on variables for changing network conditions. However, they did not consider path location, latency, speed, and energy metrics. Also, a dynamic Q-learning approach adjusted maintenance, leading to increased delays when route failures occurred without selecting alternate paths. Khan et al. [18] suggested Ant-Hocnet, a routing protocol that integrates Ant Colony Optimization (ACO) with an FL system to improve routing performance in FANETs. The FL system evaluates various link parameters like bandwidth, node mobility, and link quality to provide a comprehensive analysis. Based on these assessments, Ant-Hocnet identifies the optimal routing path. But the protocol lacks effective mechanisms to address link or path failures, which can result in decreased network throughput and higher energy consumption.

Mansour et al. [19] introduced the Cross-Layer and Energy-Aware (CLEA) with Adhoc On-demand Distance Vector (AODV) protocol to improve the FANET reliability. This method integrates the AODV protocol with cluster head selection based on Glow Swarm Optimization (GSO) and Medium Access Control (MAC) strategies. However, the protocol faces challenges with data transmission disruptions when paths break, as it lacks effective mechanisms for selecting alternative routes, resulting in diminished throughput and a lower PDR. Ren et al. [20] created a multipath routing scheme called FMQMRP, based on intuitionistic fuzzy set theory and entropy weights to optimize QoS factors. They used a cross-layer method to meet QoS requirements and find multiple transmission routes. Efficiency tables of the routes were generated using fuzzy regularization, forming a decision matrix. Factor weights were determined using information entropy, and the routes were ranked using the TOPSIS method. But network delay remains an issue due to longer path recovery times after link breaks.

Wang et al. [21] developed a novel RP called AO-AOMDV, which combines Arithmetic Optimization (AO) with the AOMDV. A fitness function was applied to evaluate multiple paths, and AO was employed to select the optimal route. However, the network lifetime was limited due to using specific parameters as routing selection criteria, which did not cover all relevant metrics. Lansky et al. [22] introduced an energy-conscious routing framework for FANETs utilizing the Optimized Link State Routing (OLSR) protocol. This approach evaluates the network quality between UAVs by analyzing hello messages and connection duration. The firefly algorithm was employed to select multipoint relays by considering residual energy, link quality, network connectivity, and UAV cooperation. Data transport pathways were identified using a mix of energy levels and network dependability. Despite these benefits, the protocol encountered connection failures and had a high routing cost.

Yang et al. [23] developed the Inter-Cluster RP (ICRP) using a hybrid ACO algorithm to select the best relay node. Inspired by Physarum polycephalum's foraging conduct, ICRP considers factors like hop count, node load, and pheromone weight. It employs predictive repair and contraction to maintain routes for UAVs' high mobility, but data loss may occur due to network link instability. Ren et al. [24] introduced an online K-means learning algorithm for dynamic clustering in UAV networks. The 3D Gauss-Markov mobility framework was used to forecast UAV locations, and K-means online learning was utilized for dynamic node clustering. Subsequently, inter-cluster forwarding nodes were selected to transmit data among clusters. However, the PDR was low since it failed to account for link/path stability, potentially affecting data transfer during connection failures. Hyd-AODV, a hybrid reactive routing system for decentralized UAV networks, was designed by Garg et al. [25]. It found routes using a multi-metric route selection algorithm, monitored an area around the chosen route, and switched to an alternate route before the current route's quality dropped below a threshold. A queue management method was also implemented to prioritize packet transfers depending on the age of the data. However, the PDR remained low, and routing overhead was considerable owing to the high mobility of UAVs.

In summary, the above-discussed studies suggest different RPs to enhance network reliability and efficiency. However, they face challenges in managing backup paths effectively, resulting in delays, reduced throughput, and higher energy usage. Efficient backup path management is crucial to minimizing overhead and optimizing network performance.

3. METHOD

This section describes the proposed route selection model designed for FANETs. HOA-MEPFL-CLCT-RP is a routing protocol that uses multiple paths and reacts to changes, supporting FANETs. The protocol incorporates FL to find numerous near-optimal routes, uses HOA to selectively apply the most feasible backup route depending on the survival probability of links, and integrates a CLCT mechanism to provide smooth failover and packet duplication. When there is a connection failure, this protocol will automatically switch to the pre-optimized backup path, and hence, the delay and control overhead will be minimized significantly. Here, the FL scheme considers input factors such as distance, mobility, energy, and delay to select a set of multiple near-optimal loop-free routes between the source UAV and the destination UAV. Meanwhile, the HOA considers the set of candidate paths as input to pick the optimal backup path based on the link survival probability as a fitness function. Thus, even in highly dynamic UAV network settings, the architectural design can guarantee high reliability, low E2D, high PDR, and high energy efficiency.

Table 1 presents the description of symbols and parameters used in this study. At time step t, a homogeneous FANET consists of N UAVs and E links, as shown in Figure 1. Each UAV, denoted as UAV i, has knowledge of its position $\mathrm{a}_i = (x_i, y_i, z_i))$ and velocity $\mathrm{v}_i = (v_{x,i}, v_{y,i}, v_{z,i})$ in three-dimensional space at t. The distance between UAVs i and j at time t, based on the Euclidean metric is expressed as $d_{ij}(t) = \|\mathrm{a}_i(t) - \mathrm{a}_j(t)\|_2$, where $\mathrm{a}_i(t)$ and $\mathrm{a}_j(t)$ denotes the positions of UAVs i and j at time t, respectively. UAV intensity will be constrained to the range $[0, V_{max}]$, where $V_{max} > 0$ is a constant. A link e_{ij} is considered part of the set E at time t if the distance $d_{ij}(t)$ is within the transmission range R, i.e., $E(t) = \{e_{ij}(t): d_{ij}(t) \leq R\}$.

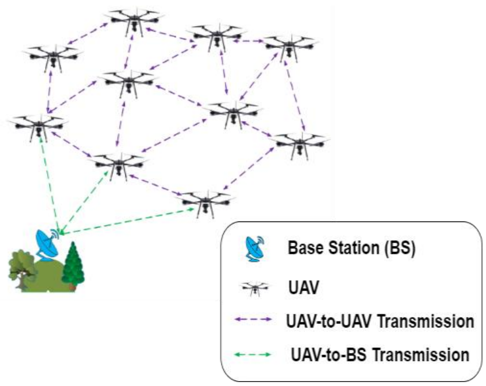

Figure 1. Architecture of FANET

Table 1. List of symbols and parameters

Symbols	Description
a_i	Position of UAV i
v_i	Velocity of UAV i
t	Time or current iteration
$d_{ij}(t)$	Euclidean distance
$\mathrm{a}_i(t)$ and $\mathrm{a}_j(t)$	Positions of UAVs i and j at t, respectively
V_{max}	Maximum velocity
e_{ij}	Link between UAV i and UAV j
R	Communication range
$p(\hat{\mathrm{a}}_i = \mathrm{a})$	PDF for each UAV's position a_i
$P(e_{ij})$	Survival probability of e_{ij}
$B_R(\mathrm{a})$	Sphere with radius R fixed at point a
s and d	Source and destination UAVs, respectively
$\mathcal{E}_{sd}$	Collection of possible routes among s and d
e^*	Optimal path from $\mathcal{E}_{sd}$
$P(\mathrm{e})$	Reliability of entire path
$\bar{\mathrm{e}}^*$	Primary path failure
$b(\mathrm{e}^*)$	Best backup path
P_i	Position of the i^{th} potential solution
$p_{i,j}$	j^{th} decision parameter associated with P_i
N	Total hippos in the population
m	Number of control parameters
$rand_{i,j}$	Random value
lb_j and ub_j	Lower and upper limits for the j^{th} decision variable, respectively
F	Vector containing the fitness values
F_i	Fitness value for the i^{th} hippo
$P_i^{M\_hippo}$	Position of the male hippo
D_hippo	Position of the dominant hippo
$rand_1, rand_2, rand_6, rand_7, Q_1, Q_2, rand_{10}, rand_{12}, rand_{13}, \tau$	Random values
I_1, I_2	Integer values between 1 and 2
$P_i^{FB\_hippo}$	Position of the female or juvenile hippo within the group
$\overrightarrow{rand}_1, \dots, \overrightarrow{rand}_4, \overrightarrow{rand}_{11}$	Random vectors
T	Maximum number of iterations
μ_i	Average value of a randomly selected hippo

h_1 and h_2	Random values
$\vec{D}$	Separation between the hippopotamus and the threat
$F_{Predator_j}$	Factor in which hippopotamus influences defensive actions
$P_i^{hippo_R}$	Position of the hippopotamus directed toward the threat
a	Random value between 2 and 4
c	Random value between 1 and 1.5
d	Random value between 2 and 3
g	Random value between -1 and 1
$\overrightarrow{rand}_9$	Erratic vector with $1 \times m$ size
$\overrightarrow{RL}$	Levy distribution
ω and v	Random values
ϑ	Constant value
Γ	Gamma function
$F_i^{hippo\_R}$	Hippopotamus has been captured and will be replaced inside the group itself
$P_i^{hippo\_E}$	Position of the hippopotamus in search of the closest secure area

3.1 Definition of Fitness Function

The Base Station (BS) does not have the precise locations of all UAVs but estimates a Probability Density Function (PDF) for each UAV's position a_i represented as $p(\hat{\mathrm{a}}_i = \mathrm{a})$. This probability distribution reflects the chance of UAV i being located at a specific point a, as estimated by the BS's approximation. The endurance likelihood of a link $P(e_{ij})$ is defined as:

$$P(e_{ij}) = P_R(d_{ij} \leq R) = \int_{B_R(0)} p(\mathrm{a}_i - \mathrm{a}_j = \mathrm{a})d\mathrm{a} \tag{1}$$

In Eq. (1), $B_R(\mathrm{a})$ represent a sphere with radius R fixed at point a. Let, e be the route from the source (s) to target (d), $\mathcal{E}_{sd}$ denotes the collection of possible routes among s and d. The FL system selects the ideal route e^* from $\mathcal{E}_{sd}$ which provides higher total probability of path persistence as defined in Eq. (2),

$$\mathrm{e}^* = \underset{\mathrm{e} \in \mathcal{E}_{sd}}{\operatorname{argmax}} P(\mathrm{e}) \tag{2}$$

If each link is considered independent, the reliability of the entire path is determined by multiplying the reliability of the individual links as $P(\mathrm{e}) = \prod_{e \in \mathrm{e}} P(e)$. Typically, loops are excluded from consideration, as they generally have a minimal effect on the overall reliability. To improve the success rate in the event of primary path failure $(\overline{\mathrm{e}}^*)$, the best backup path, $b(\mathrm{e}^*)$ as in Eq. (3) is selected from a set of alternative paths.

$$b(\mathrm{e}^*) = \underset{b \in \mathcal{E}_{sd} | \overline{\mathrm{e}}^*}{\operatorname{argmax}} P(b | \overline{\mathrm{e}}^*) \tag{3}$$

Where, $\mathcal{E}_{sd}|\overline{\mathrm{e}}^*$ refers to the set of backup routes from s to d when the primary path e^* is no longer accessible. In active environments such as rapid multi-hop FANETs, the selected primary path may become compromised. To tackle this issue, it is useful to keep a record of backup routes that can be utilized if the primary route becomes unavailable. This approach enhances the reliability of data transmission in overloaded UAV networks by establishing several ideal routes to the target nodes. Consequently, this research employs the HOA method to identify the best alternative path without introducing significant computational overhead. The HOA selects the optimal backup path based on the link survival probability in Eq. (1), which serves as the fitness function.

3.2 Design of HOA

The hippopotamus is a unique mammal found across Africa, living in rivers and wetlands in a semi-aquatic lifestyle. The HOA is inspired by three main behaviors exhibited by hippos. These include the tendency of young hippos to wander away from their group, their defensive actions when threatened and their instinct to escape danger by heading toward water. Young hippos are naturally curious and often stray, which puts them at risk of becoming prey. When confronted by predators, hippos use their powerful jaws and vocalizations to defend themselves. Due to the threat posed by their large mouths, predators such as lions and hyenas tend to avoid hippos. Additionally, when in danger, hippos instinctively flee to water, where they are more secure.

3.2.1 Mathematical Modeling for HOA

The hippos in the HOA are identified as candidate paths, and the fitness of these paths is based on the specific contraints, including the stability of links, latency, and energy efficiency. This HOA allows for the simultaneous search of many candidate routes; paths with greater link-survival probabilities, lower propagation delay, and lower energy usage are considered more consistent and represent the optimal backup path. The main working principle of HOA resembles the social, defensive, and escape behaviors of hippos to explore and optimize a candidate solution. The three different phases in this HOA are shown in Figure 2. First, HOA performs a global exploration stage, in which individuals are placed apart from or towards a dominant leader, thereby allowing the exploration of a wide range of routing options. It then uses a predator-avoidance subroutine, further refining the search on the potentially best routes, eliminating poorer ones. During the last exploitation phase, the agents go to assigned safe areas, and it will optimize the best backup path. By transforming into this sequential behavioral repertoire, HOA can isolate the most consistent backup route with minimum computational cost, hence giving resilient routing decisions in highly dynamic FANET environments.

Figure 2. Different phases in HOA

The algorithm starts by generating random initial solutions, as:

$$P_i: p_{i,j} = lb_j + rand_{ij} \cdot (ub_j - lb_j), i = 1, \dots, N;\ j = 1, \dots, m \tag{4}$$

In Eq. (4), the position of the i^{th} potential solution is denoted by P_i, while $p_{i,j}$ represents the j^{th} decision parameter associated with it. N stands for the overall values of hippos in the population and m indicates the control parameters in the optimization task. The term $rand_{i,j}$ is a randomly generated value within the interval [0,1], while lb_j and ub_j orrespond to the lower and upper limits for the j^{th} decision variable, respectively. The population of hippos is represented by the matrix (P), as shown below:

$$P = \begin{bmatrix} P_1 \\ \vdots \\ P_i \\ \vdots \\ P_N \end{bmatrix}_{N\times m} = \begin{bmatrix} p_{1,1} & \cdots & p_{1,j} & \cdots & p_{1,m} \\ \vdots & \ddots & \vdots & ⋰ & \vdots \\ p_{i,1} & \cdots & p_{i,j} & \cdots & p_{i,m} \\ \vdots & ⋰ & \vdots & \ddots & \vdots \\ p_{N,1} & \cdots & p_{N,j} & \cdots & p_{N,m} \end{bmatrix}_{N\times m} \tag{5}$$

The evaluation of fitness is based on the solutions provided by the candidate positions within the decision variable space, as given below:

$$F = \begin{bmatrix} F_1 \\ \vdots \\ F_i \\ \vdots \\ F_N \end{bmatrix}_{N\times 1} = \begin{bmatrix} F(X_1) \\ \vdots \\ F(X_i) \\ \vdots \\ F(X_N) \end{bmatrix}_{N\times 1} \tag{6}$$

In Eq. (6), F represents the vector containing the fitness values and F_i is the fitness value for the i^{th} hippo. The solution exhibiting the greatest fitness score is regarded as the best option. This best solution is revised in each iteration as the candidate solutions are updated.

Exploration (Phase 1):

A group of hippos includes adult females, young hippos, mature males and a dominant male leader. The dominant male is selected based on an objective function that either maximizes or minimizes specific parameters. For protection, hippos tend to stay close together, with the dominant male overseeing the herd's territory. Females typically surround the dominant male and once young males mature, they are driven out of the group. These expelled males must either fight for dominance or find ways to attract females. The arrangement of male hippos within the herd's environment is depicted in Eq. (7)

$$P_i^{M\_hippo}: p_{i,j}^{M\_hippo} = p_{i,j} + rand_1 \times \left(D\_hippo - I_1 p_{i,j}\right), i = 1, \dots, \left[\frac{N}{2}\right]; j = 1, \dots, m \quad (7)$$

$$h = \begin{cases} I_2 \times \overrightarrow{rand}_1 + (\sim Q_1) \\ 2 \times \overrightarrow{rand}_2 - 1 \\ \overrightarrow{rand}_3 \\ I_1 \times \overrightarrow{rand}_4 + (\sim Q_2) \\ rand_5 \end{cases} \quad (8)$$

$$\mathcal{T} = e^{\left(-\frac{t}{T}\right)} \quad (9)$$

$$P_i^{FB\_hippo}: p_{i,j}^{FB\_hippo} = \begin{cases} p_{i,j} + h_1 \times (D\_hippo - I_2 \mu_i), & T > 0.6 \\ \Xi, & Otherwise \end{cases} \quad (10)$$

$$\Xi = \begin{cases} p_{i,j} + h_2 \times \left(\mu_i - D_{hippo}\right), & rand_6 > 0.5 \\ lb_j + rand_7\left(ub_j - lb_j\right), & Otherwise \end{cases}, i = 1, \dots, \left[\frac{N}{2}\right]; j = 1, \dots, m \quad (11)$$

In Eqns. (7) – (11), $P_i^{M\_hippo}$ represents the position of the male hippo while D_hippo represents the position of the dominant hippo, as it holds the highest fitness value in the current iteration. $rand_1, rand_2, rand_6, rand_7$ are random values within the range [0,1]. I_1, I_2 are integer values between 1 and 2. $P_i^{FB\_hippo}$ represents the position of the female or juvenile hippo within the group. $\overrightarrow{rand}_1, \dots, \overrightarrow{rand}_4$ are random vectors in the range [0,1]. t denotes the current iteration and T is the maximum number of iterations. μ_i is the average value of a randomly selected hippo, with an equal likelihood of including the present hippo (P_i), Q_1, Q_2 are arbitrary integer values that can either be 0 or 1. Young hippos generally remain close to their mothers, but their natural curiosity may sometimes cause them to stray from the group. If the value of $\mathcal{T}$ exceeds 0.6, it suggests that the young hippo has ventured away from its mother, as indicated in Eq. (9). If the random value $rand_6$ is greater than 0.5, as shown in Eq. (11), it signifies that the young hippo has moved away but is either still in proximity to the herd or has become separated from the group. Eq. (10) and Eq. (11) model the movements and behaviors of immature and female hippos. h_1 and h_2 are values selected randomly from the five cases presented in Eq. (8). The process for updating the locations of male, female, or juvenile hippos inside the herd is described as follows:

$$P_i = \begin{cases} P_i^{M\_hippo}, & F_i^{M\_hippo} < F_i \\ P_i, & Otherwise \end{cases} \quad (12)$$

$$P_i = \begin{cases} P_i^{FB\_hippo}, & F_i^{FB\_hippo} < F_i \\ P_i, & Otherwise \end{cases} \quad (13)$$

In Eqns. (12) – (13), F_i represents the objective function in which h vectors in the scenarios of I_1 and I_2 boosts the global search capability and exploration within the HOA, leading to better overall efficiency.

Exploration (Phase 2):

Hippopotamuses gather in groups for protection, as their massive size helps ward off potential threats. However, younger or weaker hippos remain susceptible to predators like crocodiles, lions and hyenas. When faced with danger, hippos emit loud sounds and move toward the predator in an attempt to drive it off. The location of the predator in the environment is shown below:

$$Predator: Predator_j = lb_j + \overrightarrow{rand}_8 \times \left(ub_j - lb_j\right), j = 1, \ldots, m \tag{14}$$

In Eq. (14), $\overrightarrow{rand}_8$ denotes the random vector with values that fall between 0 and 1.

$$\vec{D} = \left|Predator_j - p_{i,j}\right| \tag{15}$$

In Eq. (15), $\vec{D}$ represents the separation between the hippopotamus and the threat. At this point, the hippopotamus demonstrates defensive actions influenced by the factor $F_{Predator_j}$ to safeguard itself. If $F_{Predator_j}$ is less than F_i, suggesting the predator is very nearby, the hippopotamus quickly faces the threat and advances toward it to encourage retreat. If $F_{Predator_j}$ exceeds F_i the hippopotamus turns toward the predator with restricted movement, signaling its presence within its domain.

$$P_i^{hippo_R}: p_{i,j}^{hippo_R} = \begin{cases} \overrightarrow{RL} \oplus Predator_j + \left(\frac{a}{c - d \times \cos(2\pi g)}\right) \times \left(\frac{1}{\vec{D}}\right), & F_{Predator_j} < F_i \\ \overrightarrow{RL} \oplus Predator_j + \left(\frac{a}{c - d \times \cos(2\pi g)}\right) \times \left(\frac{1}{2\vec{D} + \overrightarrow{rand}_9}\right), & F_{Predator_j} \geq F_i \end{cases}$$

$$i = \left[\frac{N}{2}\right] + 1, \left[\frac{N}{2}\right] + 2, \ldots, N; j = 1, \ldots, m \tag{16}$$

In Eq. (16), $P_i^{hippo_R}$ signifies the position of the hippopotamus directed toward the threat, a denotes a random value ranging among 2 and 4, c devises the randomly selected number between 1 and 1.5, d provides the Spontaneous value among 2 and 3, g is an arbitrary integer between -1 and 1, $\overrightarrow{rand}_9$ refers to a erratic vector with $1 \times m$ size and $\overrightarrow{RL}$ represents a Levy distribution applied to model sudden shifts in the attacker 's location during an assault on the hippopotamus. The Levy movement pattern is outlined as:

$$\mathcal{L}evy(\vartheta) = 0.05 \times \left(\frac{\omega \times \sigma_\omega}{|v|^{\frac{1}{\vartheta}}}\right) \tag{17}$$

$$\sigma_\omega = \left[\frac{\Gamma(1+\vartheta)\sin\left(\frac{\pi\vartheta}{2}\right)}{\Gamma\left(\frac{(1+\vartheta)}{2}\right)\vartheta 2^{\frac{(\vartheta-1)}{2}}}\right]^{\frac{1}{\vartheta}} \tag{18}$$

In Eqns. (17) & (18), ω and v are stochastic values within the interval $[0,1]$, ϑ is a fixed value (ϑ=1.5) and Γ denotes the Gamma function. As described in Eq. (19), if $F_i^{hippo\_R}$ signifies the the hippopotamus has been captured and will be replaced inside the group itself. Otherwise, the predator will flee and the hippopotamus will rejoin their respective group. The global exploration stage exhibits significant enhancement in the second stage, collaborating within the first phase to avoid falling into local optima.

$$P_i = \begin{cases} P_i^{hippo\_R}, & F_i^{hippo\_R} < F_i \\ P_i, & F_i^{hippo\_R} \geq F_i \end{cases} \tag{19}$$

Exploitation (Phase 3):

In certain scenarios, if the hippo faces a group of predators or cannot find them off, it will attempt to flee by moving towards the nearest water body, like a lake or pond, as animals such as lions and hyenas generally steer clear of water. This behavior is simulated by selecting a random position near the current location of the hippopotamus, as outlined in Eqns. (20) - (23). If the new position results in a higher objective value, it suggests that the hippo has found a protective zone and has moved there.

$$lb_j^{local} = \frac{lb_j}{t}, ub_j^{local} = \frac{ub_j}{t}, \text{ where } t = 1, \dots, T \tag{20}$$

$$P_i^{hippo\_E} : p_{i,j}^{hippo\_E} = p_{i,j} + rand_{10} \times \left(lb_j^{local} + \tau\left(ub_j^{local} - lb_j^{local}\right)\right), i = 1, \dots, N; j = 1, \dots, \tag{21}$$

In Eq. (21), $P_i^{hippo\_E}$ represents the position of the hippopotamus in search of the closest secure area, while τ is a random vector selected from one of three possible cases s in Eq. (22).

$$s = \begin{cases} 2 \times \overrightarrow{rand}_{11} - 1 \\ rand_{12} \\ rand_{13} \end{cases} \tag{22}$$

In Eq. (22), $\overrightarrow{rand}_{11}$ denotes a stochastic vector with values in the range of 0 to 1, while $rand_{10}$ and $rand_{13}$ are generated random values within the interval of 0 to 1. Furthermore, $rand_{12}$ is a randomly distributed value that follows a normal distribution.

$$P_i = \begin{cases} P_i^{hippo\_E}, & F_i^{hippo\_E} < F_i \\ P_i, & F_i^{hippo\_E} \geq F_i \end{cases} \tag{23}$$

In every cycle of the HOA, each member of the population is revised based on Stages 1 to 3 using Eqns. (7) – (23) until the last cycle. The best solution is continuously monitored and stored. At the end of the process, the dominant hippopotamus solution, representing the most favorable candidate, is identified as the final result.

Algorithm 1 HOA for optimal backup path selection

Input: Selected paths e^* from the FL system

Output: Best alternative path $b(\mathrm{e}^*)$

```
Start
//Initialization phase
Set the number of hippopotamus (N), where N = e*;
Define the highest number of iteration (T);
Generate the initial location of each hippopotamus using Eq. (4);
For each hippo, calculate the fitness function (link endurance likelihood in Eq. (1));
while(t ≤ T)
//Exploration phase (Social behavior)
 Adjust the superior hippopotamus location using the fitness value criteria;
 for (i = 1: N/2)
  Calculate the new position for i^th hippopotamus using Eqns. (7) & (10);
  Update the i^th hippo's position using Eqns. (12) & (13);
 end for
//Exploration phase (Defensive behavior)
 for (i = 1 + N/2 : N)
  Generate the random position for attackers by Eq. (14);
  Calculate the new position for i^th hippopotamus using Eq. (16);
  Update the i^th hippo's location by Eq. (19);
 end for
//Exploitation phase (Escaping behavior)
 Compute new bounds for decision parameters using Eq. (20);
 for(i = 1: N)
  Obtain the new position for i^th hippopotamus by Eq. (21);
  Revise the i^th hippo's place by Eq. (23);
 end for
 Save the best candidate solution determined so far;
end while
```

24. **Return** the ideal alternative path found by HOA
25. **End**

Algorithm 2 HOA-MEPFL-CLCT-based RP

Input: Set of UAV_i, where $i = 1, \dots, N,\ N$ denotes the total number of UAVs, data expiry time $(Exp.T_{Data})$

Output: Efficient path between the source UAV (UAV_S) and target UAV (UAV_D)

1. **Start**
2. UAV_S Produces an RREQ packet and sends it to its neighboring UAVs.
3. $\boldsymbol{if}(UAV_i\ receives\ the\ RREQ\ message\ from\ neighboring\ UAV)$
4. $\boldsymbol{if}(the\ RREQ\ message\ is\ not\ a\ duplicate)$
5. UAV_i computes its score based on the earlier-hop UAV, revises a limited RREQ packet and forwards them to the neighboring UAVs;
6. $\boldsymbol{end\ if}$
7. UAV_i determines its score based on the prior-hop UAVs, selects the UAV with highest values that suits to the previous hop UAV, and sends the values to the nearby UAVs;
8. $\boldsymbol{end\ if}$
9. $\boldsymbol{if}(UAV_D\ receives\ the\ RREQ\ message)$
10. UAV_D estimates its score, updates the RREQ packets, and finds the near-best routes by the FL;
11. Perform **Algorithm 1** to choose the best backup routes;
12. $\boldsymbol{if}(link\ failure\ exists)$
13. Apply the best secondary route for communication;
14. $\boldsymbol{else}$
15. **Go to** Step 3;
16. $\boldsymbol{end\ if}$
17. $\boldsymbol{end\ if}$
18. UAV_D produces an RREP packet and exceeds them to the former-hop UAV via the selected routes;
19. $\boldsymbol{while}(ID\ of\ UAV_i \neq Source\ IP\ Address\ field\ of\ the\ RREP\ message)$
20. The incoming UAV_i checks its routing table for the next hop and then multicasts the RREP via the chosen multiple paths to the previous-hop UAV.
21. $\boldsymbol{end\ while}$
22. UAV_S sends data packets to UAV_D via the selected multiple paths;
23. $\boldsymbol{for}(i = 1{:}N)$
24. $\boldsymbol{if}\left(E_{UAV_i} < E_{threshold}\ or\ Traffic_{UAV_i} < Traffic_{threshold}\ or\ Q_{link_{i-j}} < Q_{threshold}\right)$
25. UAV_i sends a caution information to the former-hop UAV $\left(UAV_j\right)$;
26. UAV_j selects the nearby UAV adjacent (that has not yet been chosen) to UAV_i as $UAV_{alternative}$;
27. $\boldsymbol{if}(UAV_{alternative}\ cannot\ create\ a\ valid\ path)$
28. Apply the best substitute route to send the data packets;
29. $\boldsymbol{end\ if}$
30. $\boldsymbol{end\ if}$
31. $\boldsymbol{if}(UAV_{alternative}\ created\ a\ valid\ path\ \ \&\&\ Exp.T_{Data} == false)$
32. Add $UAV_{alternative}$ as its consequent hop UAV in the transmitting table;
33. Transfer the data packets using the new path;
34. $\boldsymbol{else\ if}(Exp.T_{Data}True\&\&UAV_{alternative}\ cannot\ create\ a\ valid\ path)$
35. Perform the CLCT algorithm [8];
36. $\boldsymbol{end\ if}$
37. Verify if $UAV_{alternative}$ is designated as the best UAV or possible UAV is ID;
38. Forward the data packets through the ideal route;
39. Else, transmit derivative packets to $UAV_{alternative}$ from the ideal UAV or latent UAV;
40. Communicate the data packs over the alternative route;
41. $\boldsymbol{end\ for}$
42. UAV_S forwards a path authentication data to UAV_D;
43. $\boldsymbol{if}(path\ is\ valid)$

44. UAV_D relays an ACK message to UAV_S;
45. $\boldsymbol{else}$
46. UAV_S gets back the Route Error (RRER) information from the midway UAV;
47. **Return** to Step 2;
48. $\boldsymbol{end\ if}$
49. **End**

Thus, th HOA-enriched multipath routing protocol with FL significantly improves the FANET performance by enabling the selection of highly reliable backup paths. This can alleviate delays, reduce routing overhead, and enhance path stability, even in the dynamic changing network environments.

4. RESULTS

The proposed model HOA-MEPFL-CLCT-RP is assessed by comparing it to existing routing protocols such as MEPFL-CLCT-RP [8], Ant-Hocnet [10], FMQMRP [12], and AO-AOMDV [13]. Both the proposed and current models are evaluated in the Network Simulator (NS-2.35) platform, which is installed on an Ubuntu platform with the variables detailed in Table 2. A comprehensive comparison is performed by analyzing factors like E2D, PDR, routing overhead, path stability, hop count, and energy consumption.

Table 2. List of simulation parameters

Parameters	Range
Simulation platform	NS-2.35
Simulation duration	350 seconds
UAVs speed	m/s
Mobility model	Random waypoint
MAC layer	IEEE 802.11a
No. of UAVs	120
Simulation area	1500×1500×1000 m3
Starting UAV energy	2100 J
Transmission range	310 m
Packet size	1 Kbit
Type of path loss	Free-space

4.1 E2D

It represents the mean duration for the source UAV to deliver data to the destination target UAV. Figure 3 displays E2D values of both suggested and existing protocols for various UAV quantities. It is shown that that HOA-MEPFL-CLCT-RP effectively lowers E2D by intelligently choosing alternative paths to avoid network relation disasters during data communication. When it comes to addressing connection failures that lead to reduced E2D, HOA-MEPFL-CLCT-RP outperforms other protocols. A case in point is the E2D reduction achieved by HOA-MEPFL-CLCT-RP with 120 UAVs, which is 73.17% lower than FMQMRP, 70.27% lower than AO-AOMDV, 64.52% lower than Ant-Hocnet, and 26.67% lower than MEPFL-CLCT-RP.

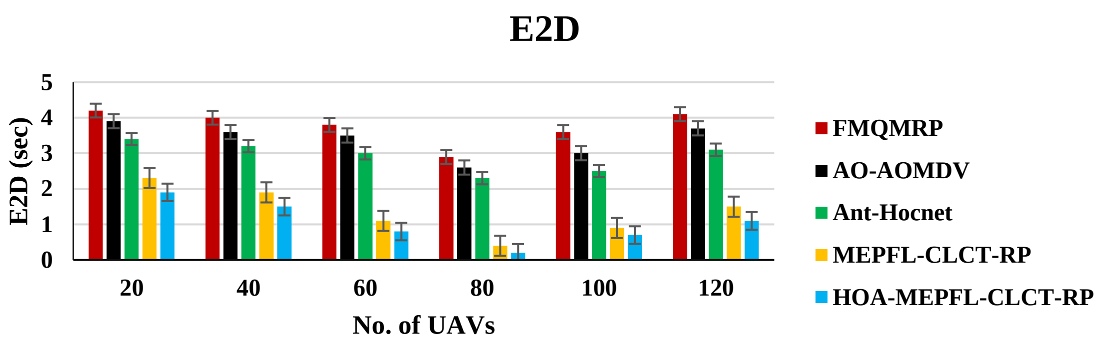

Figure 3. Compression of E2D with No. of UAVs

4.2 PDR

It shows what proportion of data the target UAV out of the total data that was produced received. Figure 4 compares the PDR of HOA-MEPFL-CLCT-RP to other existing techniques for varying numbers of UAVs. The results demonstrate that HOA-MEPFL-CLCT-RP significantly enhances PDR with increasing UAV numbers through the mitigation of link failures and the utilization of suitable backup routes. Compared to FMQMRP, AO-AOMDV, Ant-Hocnet, and MEPFL-CLCT-RP, HOA-MEPFL-CLCT-RP improves PDR in a 120 UAV network by 31.94%, 26.67%, 17.28%, and 2.15%, respectively.

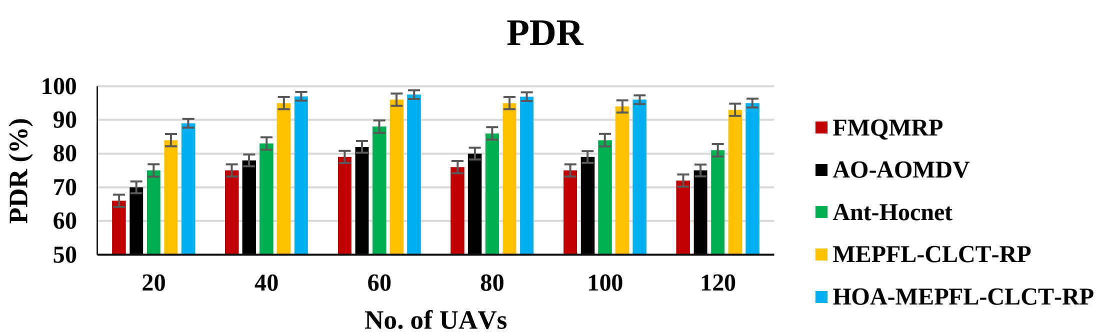

Figure 4. Comparsion of PDR with No. of UAVs

4.3 ROUTING OVERHEAD

This metric measures the success rate of the packet forwarding operation in reaching the target UAV.

Figure 5 shows a comparison of the routing overhead for several protocols with different numbers of UAVs in the network. To ensure dependable data transfer, HOA-MEPFL-CLCT-RP chooses the best backup routes, which significantly lowers routing overhead. When compared to FMQMRP, AO-AOMDV, Ant-Hocnet, MEPFL-CLCT-RP, and others, HOA-MEPFL-CLCT-RP lowers routing overhead in a 120 UAV network by 36.03%, 26.83%, 18.92%, and 9.91%, respectively. In dynamic situations with a high density of UAVs, minimizing control messages is crucial for improving FANET performance, leading to faster and more reliable network operations.

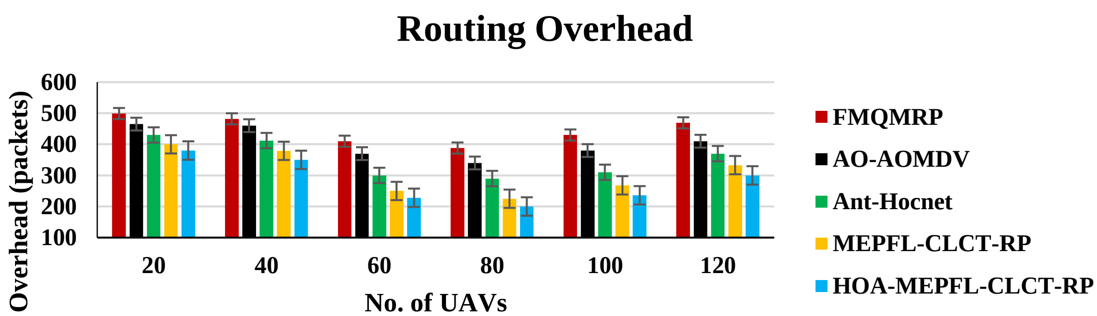

Figure 5. Analysis of routing overhead with No. of UAVs

4.4 PATH STABILITY

It is quantified by adding up all the paths that end up failing. Path resilience is improved as the number of unsuccessful routes decreases.

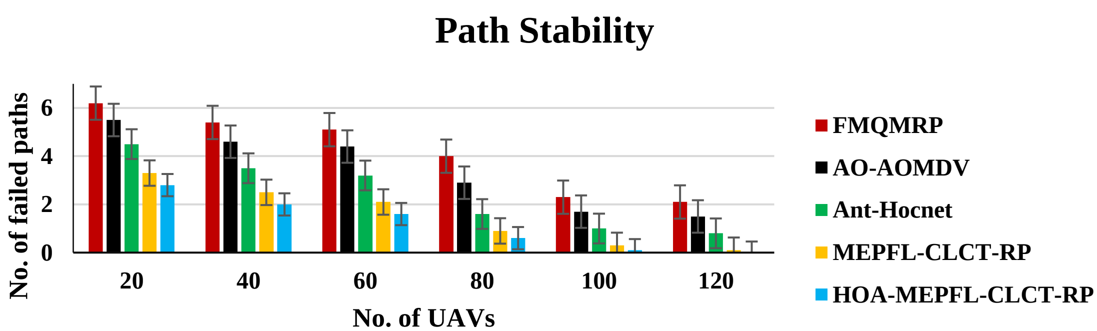

Figure 6. Analysis of path stability with No. of UAVs

Figure 6 shows the results of several RPs for route stability with varied quantities of UAVs. In contrast to competing protocols, HOA-MEPFL-CLCT-RP maintains fully functional paths even with 120 UAVs in the network. For a network of 20 UAVs, the reduction in the number of failed paths is 54.84%, 49.09%, 37.78%, and 15.15% compared to FMQMRP, AO-AOMDV, Ant-Hocnet, and MEPFL-CLCT-RP, respectively. Proof that HOA-MEPFL-CLCT-RP can keep routes stable, a need for FANET data transmission reliability. It enhances network dependability and efficiency by selecting optimal backup channels in scenarios with a high density of UAVs or across long distances.

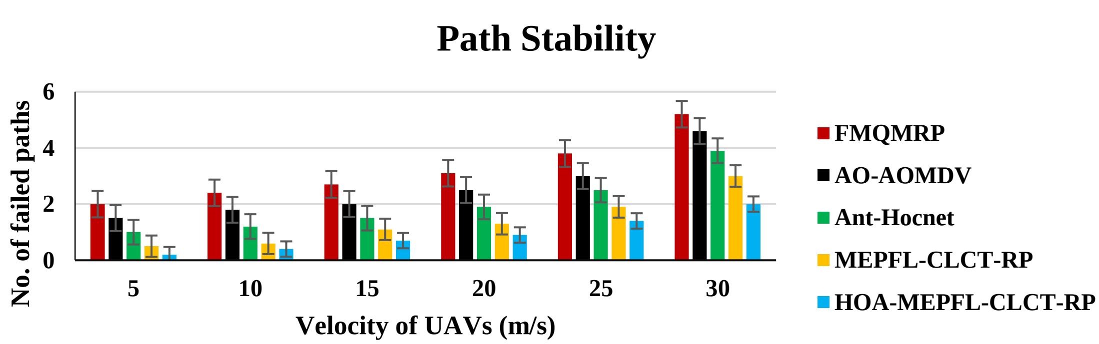

Figure 7. Comparison of path stability with velocity of UAVs

During data transmission at various UAV velocities, Figure 7 compares route stability across different RPs. By drastically cutting down on unsuccessful pathways, HOA-MEPFL-CLCT-RP surpasses the other RPs, especially when

UAV speeds are greater. The number of unsuccessful pathways is reduced by 61.54%, 56.52%, 48.72%, and 33.33% at a speed of 30 m/s by HOA-MEPFL-CLCT-RP in comparison to FMQMRP, AO-AOMDV, Ant-Hocnet, and MEPFL-CLCT-RP, respectively.

4.5 HOP COUNT

It is a measure of the typical number of intermediate nodes in the data transmission path. The hop counts during data transmission with various routing protocols (RPs) and varied node transmission ranges are compared in Figure 8. By cutting down on routing hops, HOA-MEPFL-CLCT-RP achieves better performance than the competition, especially at longer transmission distances. The number of hops decreased by 81.58%, 76.67%, 65%, and 36.36% at a range of 500 m for HOA-MEPFL-CLCT-RP compared to FMQMRP, AO-AOMDV, Ant-Hocnet, and MEPFL-CLCT-RP, accordingly.

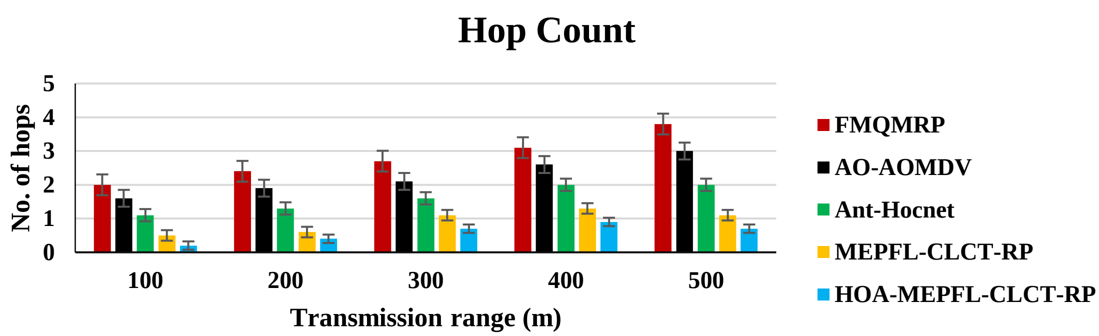

Figure 8. Hop count vs. transmission range

4.6 Energy Consumption

It finds out how much power each UAV used up at the end of the route construction and data transmission operation.

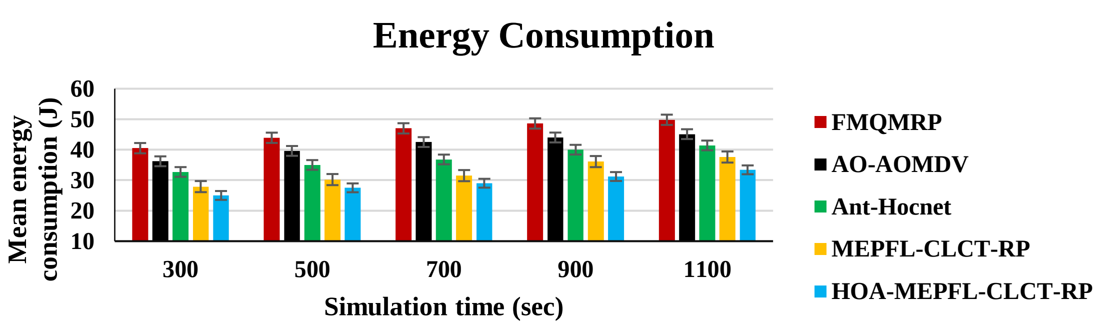

Figure 9 Analysis of energy utilization with simulation time

The energy usage during data transmission for several RPs with varied simulation periods is compared in Figure 9. When compared to FMQMRP, AO-AOMDV, Ant-Hocnet, and MEPFL-CLCT-RP at 1300 seconds, HOA-MEPFL-CLCT-RP demonstrates superior energy efficiency, reducing energy use by 31.45%, 25.79%, 18.18%, and 9.54%, respectively. In order to accomplish these cost reductions, the protocol minimizes control overhead, uses optimum backup pathways to decrease retransmissions, and selects routes efficiently. Reduced power consumption in UAV networks is largely attributable to these elements. The HOA-MEPFL-CLCT-RP reduces energy consumption, which increases the endurance of energy-limited FANETs, allowing for longer mission durations and greater performance in UAV networks for diverse applications.

4.7 Sensitivity analysis for HOA

Figure 10 illustrates the sensitivity of the HOA parameters, including population size and the number of iterations, in terms of the convergence curve. The findings have shown that the optimal fitness achieved by HOA declines more rapidly as the population size increases to 40 and 80, indicating that optimization is faster and the search is more efficient. Larger populations reach lower levels of fitness faster, demonstrating high exploration ability. However, the curve remains flat beyond 40 individuals, indicating a decrease in returns. This suggests that a moderate population size (around 40) offers a satisfactory trade-off between the convergence rate and the computation cost.

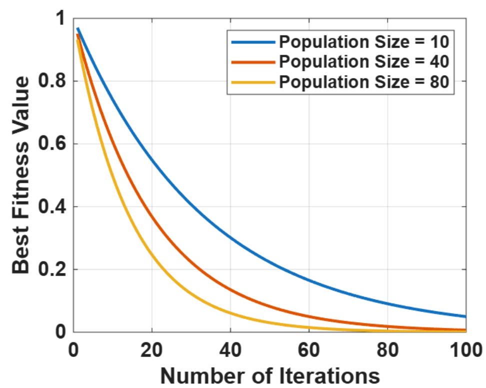

Figure 10. Convergence curve for HOA

4.8 Trade-off between HOA complexity and performance gain

Compared to simpler protocols like AODV or OLSR, the HOA-MEPFL-CLCT-RP imposes a significant computational load on the HOA and the execution of FL, as it requires more CPU cycles and memory than simple protocols. Despite this increased complexity, the protocol provides high performance, with reductions in E2D of between 20-73%, increases in PDR of between 2 and 32%, and a reduction in routing overhead of between 10 and 36%. At the same time, it provides stability in paths with high node mobility. Because modern UAV processors now have sufficient computational resources to meet these needs, the resultant trade-off favors important FANET applications where reliability and low latency are the most critical factors, rather than the related computational costs.

4.9 Statistical anlaysis for HOA-MEPFL-CLCT-RP and existing RPs

Table 3. Results of pairwise 2-tailed t-tests across all metrics

Protocols	t-value	df	Mean±SD	Sig. (2-tailed)
HOA-MEPFL-CLCT-RP vs. FMQMRP	22.69	12	2.98±0.24	0.0002
HOA-MEPFL-CLCT-RP vs. AO-AOMDV	18.56	12	2.23±0.19	0.0001
HOA-MEPFL-CLCT-RP vs. Ant-Hocnet	14.43	12	1.54±0.09	0.0001
HOA-MEPFL-CLCT-RP vs. MEPFL-CLCT-RP	6.91	12	1.12±0.04	0.0000

Table 3 shows the outcomes of the pairwise two-tailed t-tests between the proposed HOA-MEPFL-CLCT-RP and existing protocols in all of the performance metrics. It is found that the proposed protocol has a significantly higher level of superiority ($p < 0.001$) than FMQMRP, AO-AOMDV, Ant-Hocnet, and MEPFL-CLCT-RP; t-values range from 6.91 to 22.69. The results demonstrate that the improvements in performance are statistically significant.

5. DISCUSSION

This section discusses the real-world deployment feasibility and hardware constraints. The HOA-based routing scheme enhances the reliability of the UAV swarms by allowing autonomous choice of the UAVs to find stable backup paths at a very low computational cost. So, swarm systems can maintain high connectivity during dynamic processes, such as surveillance or disaster-response operations. Rapidly adapting to topological changes and switches in the quality of links, HOA supports decentralized, resilient communication. However, the viability of implementing the proposed HOA-MEPFL-CLCT-RP essentially depends on the computational and communication capabilities of typical available UAV platforms. Due to its dependence on FL assessment, link survival estimation, and HOA-based optimization, this protocol requires average onboard processing capabilities but is also suitable for lightweight UAVs, which have access to standard embedded processors. The routing functions cause the least auxiliary control overhead, making them feasible with UAVs with limited battery capacities, assuming the use of energy-efficient communication devices, e.g., IEEE 802.11a or similar standards. However, real-life implementation should consider the hardware requirements, such as limited memory to store multiple candidate routes, limited GPS accuracy that could potentially worsen link quality prediction, and unreliable sensors that can impact mobility and position reporting. Therefore, it is necessary to have a stable range of communication, sufficient battery supply, and strong sensing modules to guarantee reliable real-time routing execution in working FANET settings.

Furthermore, in real-life implementation of FANETs, the HOA-MEPFL-CLCT-RP can have failure modes where the topology change is faster than the protocol can re-estimate link survival, leading to a situation in which paths are sometimes chosen suboptimally, or backup paths are not activated in time. Scalability is also limited with enormous UAV swarms because the maintenance of multiple candidate paths, as well as the fitness analysis of these candidate paths, may increase control overhead and cause extra processing loads on resource-limited nodes. Higher mobility can also compromise the resilience of route maintenance behavior due to frequent link breakages and also due to the rapid changes in the distance between inter-UAVs, requiring more frequent re-optimization and possibly increasing transient delay. However, the joint use of FL and HOA-based optimization offers the resilience of providing continuous adjustment to network dynamics, although additional tuning might be needed to ensure uniform functionality under very dense and highly mobile FANET conditions.

6. CONCLUSION

In this paper, the proposed HOA-MEPFL-CLCT-RP for FANETs uses a FL system to find several almost optimal paths between source and destination nodes. Then, using the link survival probability, the HOA determines which path is the best fit and uses it as a backup. If a link fails, the source node can switch to the backup path for data transfer, reducing routing overhead and delay in dynamic FANET environments. The simulation results showed that the HOA-MEPFL-CLCT-RP outperformed traditional routing protocols in FANETs, with an average energy consumption of 30.2J, 1.03 seconds of E2D, a 95.23% PDR, 282.3 packets of overhead, 1 failed path, 0.58 hops, and an average energy consumption of 30.2J.

References

1. N. S. Labib, M. R. Brust, G. Danoy, and P. Bouvry, “The rise of drones in internet of things: a survey on the evolution, prospects and challenges of unmanned aerial vehicles,” IEEE Access, vol. 9, pp. 115466–115487, 2021, doi: 10.1109/ACCESS.2021.3104963.
2. H. Xu et al., “A survey on UAV applications in smart city management: challenges, advances, and opportunities,” IEEE J. Sel. Top. Appl. Earth Obs. Remote Sens., vol. 16, pp. 8982-9010, 2023, doi: 10.1109/JSTARS.2023.3317500.
3. A. Hussain, S. Li, T. Hussain, X. Lin, F. Ali, and A. A. AlZubi, “Computing challenges of UAV networks: a comprehensive survey,” Comput. Mater. Contin., vol. 81, no. 2, pp. 1999-2051, 2024, doi: 10.32604/cmc.2024.056183.
4. S. A. Hasan, M. A. Mohammed, and S. K. Sulaiman, “Flying ad-hoc networks (FANETs): review of communications, challenges, applications, future direction and open research topics,” in ITM Web Conf., 2024, vol. 64, p. 01002, doi: 10.1051/itmconf/20246401002
5. G. Amponis, T. Lagkas, P. Sarigiannidis, V. Vitsas, P. Fouliras, and S. Wan, “A survey on FANET routing from a cross-layer design perspective,” J. Syst. Archit., vol. 120, p. 102281, 2021, doi: 10.1016/j.sysarc.2021.102281.
6. K. Telli, et al., “A comprehensive review of recent research trends on unmanned aerial vehicles (uavs),” Syst., vol. 11, no. 8, p. 400, 2023, doi: 10.3390/systems11080400.
7. I. Chandran and K. Vipin, K. “Multi-UAV networks for disaster monitoring: challenges and opportunities from a network perspective,” SN Comput. Sci., vol. 5, p. 519, 2024, doi: 10.1007/s42979-024-02788-3.
8. I. Munasinghe, A. Perera, and R. C. Deo, “A comprehensive review of uav-ugv collaboration: advancements and challenges,” J. Sens. Actuator Netw., vol. 13, no. 6, p. 81, 2024, doi: 10.3390/jsan13060081.
9. F. Noor, M. A. Khan, A. Al-Zahrani, I. Ullah, and K. A. Al-Dhlan, “A review on communications perspective of flying ad-hoc networks: key enabling wireless technologies, applications, challenges and open research topics,” Drones, vol. 4, no. 4, p. 65, 2020, doi: 10.3390/drones4040065.
10. S. Javaid, et al., “Communication and control in collaborative UAVs: recent advances and future trends,” IEEE Trans. Intell. Transp. Syst., vol. 24, no. 6, pp. 5719-5739, 2023, doi: 10.1109/TITS.2023.3248841.
11. A. H. Wheeb, R. Nordin, A. A. Samah, M. H. Alsharif, and M. A. Khan, “Topology-based routing protocols and mobility models for flying ad hoc networks: a contemporary review and future research directions,” Drones, vol. 6, no. 1, p. 9, 2021, doi: 10.3390/drones6010009.
12. M. K. Banafaa, et al., “A comprehensive survey on 5G-and-beyond networks with UAVs: applications, emerging technologies, regulatory aspects, research trends and challenges,” IEEE Access, vol. 12, pp. 7786-7826, 2024, doi: 10.1109/ACCESS.2023.3349208.

13. N. Mansoor, M. I. Hossain, A. Rozario, M. Zareei, and A. R. Arreola, “A fresh look at routing protocols in unmanned aerial vehicular networks: a survey,” IEEE Access, vol. 11, pp. 66289–66308, 2023, doi: 10.1109/ACCESS.2023.3290871.
14. K. B. Samuel, S. D. Wolthusen, J. S. Otim, R. N. Akol, and M. Nsabagwa, “Routing protocols and mobility predictions for UAV data collection from agricultural sites: a survey,” IEEE Access, vol. 13, pp. 108626-108640, 2025, doi: 10.1109/ACCESS.2025.3582163.
15. S. W. Lee et al., “An energy-aware and predictive fuzzy logic-based routing scheme in flying ad hoc networks (FANETs),” IEEE Access, vol. 9, pp. 129977–130005, 2021, doi: 10.1109/ACCESS.2021.3111444.
16. H. Shaleena and K. Sumangala, “Multiple route selection for avoiding single point failure in flying ad hoc network (FANET),” Int. J. Comput. Netw. Appl., vol. 11, no. 3, pp. 363–374, 2024, doi: 10.22247/ijcna/2024/23.
17. M. Y. Arafat and S. Moh, “A Q-learning-based topology-aware routing protocol for flying ad hoc networks,” IEEE Internet Things J., vol. 9, no. 3, pp. 1985–2000, 2021, doi: 10.1109/JIOT.2021.3089759.
18. S. Khan, M. Z. Khan, P. Khan, G. Mehmood, A. Khan, and M. Fayaz, “An ant-Hocnet routing protocol based on optimized fuzzy logic for swarm of UAVs in FANET,” Wirel. Commun. Mob. Comput., vol. 2022, no. 1, p. 6783777, 2022, doi: 10.1155/2022/6783777.
19. H. S. Mansour et al., “Cross-layer and energy-aware AODV routing protocol for flying ad-hoc networks,” Sustain., vol. 14, no. 15, p. 8980, 2022, doi: 10.3390/su14158980.
20. P. Ren, R. Zhang, and S. Luo, “Multipath route optimization with multiple QoS constraints based on intuitionistic fuzzy set theory,” Wirel. Commun. Mob. Comput., vol. 2023, no. 1, p. 6318433, 2023, doi: 10.1155/2023/6318433.
21. H. Wang, Y. Li, Y. Zhang, T. Huang, and Y. Jiang, “Arithmetic optimization AOMDV routing protocol for FANETs,” Sens., vol. 23, no. 17, p. 7550, 2023, doi: 10.3390/s23177550.
22. J. Lansky et al., “An energy-aware routing method using firefly algorithm for flying ad hoc networks,” Sci. Rep., vol. 13, no. 1, p. 1323, 2023, doi: 10.1038/s41598-023-27567-7.
23. S. Yang et al., “Hybrid ant colony-based inter-cluster routing protocol for FANET,” Sci. Rep., vol. 14, no. 1, p. 15632, 2024, doi: 10.1038/s41598-024-64454-1.
24. Z. Ren, K. Hussain, and M. Faheem, “K-means online-learning routing protocol (K-MORP) for unmanned aerial vehicles (UAV) adhoc networks,” Ad Hoc Netw., vol. 154, p. 103354, 2024, doi: 10.1016/j.adhoc.2023.103354.
25. S. Garg, A. Ihler, E. S. Bentley, and S. Kumar, “A hybrid reactive routing protocol for decentralized UAV networks,” IEEE Trans. Aerosp. Electron. Syst., vol. 61, no. 5, pp. 11683-11701, 2025, doi: 10.1109/TAES.2025.3570276.

BIOGRAPHIES OF AUTHORS

	**H. Shaleena** holds a Bachelor of Science degree in Computer Science from Avinashilingam Deemed University, Coimbatore (2003–2006). She pursued her Master of Computer Applications (MCA) and Master of Philosophy (M.Phil.) in Computer Science at colleges affiliated with Bharathiar University during the academic years 2006–2009 and 2012–2014, respectively. She is currently pursuing her Ph.D. in Computer Science at Bharathiar University. She can be contacted at **email: shellumolmca@gmail.com**
	**K. Sumangala** is a Research Supervisor and Associate Professor in the Department of Computer Applications at Kongunadu Arts and Science College, Coimbatore. She brings over 25 years of teaching experience and more than 15 years of research experience to her academic and scholarly pursuits. She can be contacted at **email: sumangalak_ca@kongunaducollege.ac.in**